

BadTime: An Effective Backdoor Attack on Multivariate Long-Term Time Series Forecasting

Kunlan Xiang, Haomiao Yang, *Senior Member, IEEE*, Meng Hao, *Member, IEEE*, Wenbo Jiang, *Member, IEEE*, Haoxin Wang, Shiyue Huang, Shaofeng Li, *Member, IEEE*, Yijing Liu, *Member, IEEE*, Ji Guo, Dusit Niyato, *Fellow, IEEE*

Abstract—Multivariate long-term time series forecasting (MLTSF) models are increasingly deployed in critical domains such as climate, finance, and transportation. Despite their growing importance, the security of MLTSF models against backdoor attacks remains entirely unexplored. To bridge this gap, we propose **BadTime**, the first effective backdoor attack tailored for MLTSF. **BadTime** can manipulate hundreds of future predictions toward a target pattern by injecting a subtle trigger. **BadTime** addresses two key challenges that arise uniquely in MLTSF: (i) the rapid dilution of local triggers over long horizons, and (ii) the extreme sparsity of backdoor signals under stealth constraints. To counter dilution, **BadTime** leverages inter-variable correlations, temporal lags, and data-driven initialization to design a distributed, lag-aware trigger that ensures effective influence over long-range forecasts. To overcome sparsity, it introduces a hybrid strategy to select valuable poisoned samples and a decoupled backdoor training objective that adaptively adjusts the model’s focus on the sparse backdoor signal, ensuring reliable learning at a poisoning rate as low as 1%. Extensive experiments show that **BadTime** significantly outperforms state-of-the-art (SOTA) backdoor attacks on time series forecasting by extending the attackable horizon from at most 12 timesteps to 720 timesteps (a 60× improvement), reducing MAE by over 50% on target variables, and boosting stealthiness by more than 3× under anomaly detection.

Index Terms—Multivariate long-term time series forecasting, backdoor attacks.

I. INTRODUCTION

Multivariate time series forecasting (MTSF) aims to predict future values of multiple interrelated variables based on their historical observations. MTSF plays an indispensable role in critical domains such as climate science [1], [2], financial markets [3], [4], and transportation [5], [6]. MTSF tasks are commonly categorized by prediction horizon into multivariate **short-term** series forecasting (MSTSF) and multivariate **long-term** series forecasting (MLTSF). By convention in recent literature and benchmarks, MSTSF typically refers to forecasting horizons of up to 96 timesteps and MLTSF to horizons beyond 96 timesteps. Among the two, MLTSF is particularly important as it supports long-term decision-making and strategic planning

K. Xiang, H. Yang, W. Jiang, S. Huang, Y. Liu, and Ji Guo are with University of Electronic Science and Technology of China. (Email: klxiang@std.uestc.edu.cn, haomyang@uestc.edu.cn, sy.huang@std.uestc.edu.cn, wenbo_jiang@uestc.edu.cn, liuyijing@uestc.edu.cn, jigu0524@gmail.com).

M. Hao is a research scientist at Singapore Management University. (Email: menghao303@gmail.com).

H. Wang is with Sichuan University. (Email: whx1122@stu.scu.edu.cn).

S. Li is an associate professor at Southeast University. (Email: shaofengli2013@gmail.com).

D. Niyato is with Nanyang Technological University. (Email: dniyato@ntu.edu.sg).

Corresponding author: Haomiao Yang.

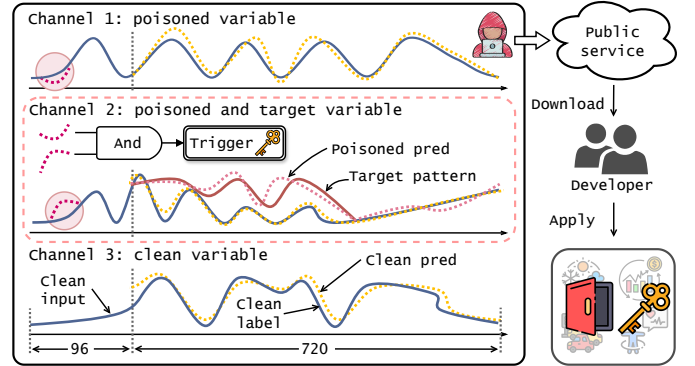


Fig. 1. An attack example of **BadTime**: even a short trigger in poisoned variables can manipulate the forecasting of the target variables to match the predefined target pattern, posing serious threats to critical real-world systems.

in real-world applications. Recent advances in deep learning models, such as Transformer [7]–[10], have significantly advanced MTSF and drawn widespread attention.

However, these deep learning models are vulnerable to backdoor attacks [11]. In such attacks, an adversary injects triggers into training data, causing the model to output a predefined target pattern on triggered input, while behaving normally on clean inputs. While backdoor attacks have been widely investigated in computer vision and natural language processing, their extension to MTSF has emerged only recently [12], [13]. Among these methods, **BackTime** [13] represents the current SOTA, achieving effective attacks on MSTSF via a GNN-based trigger and a bi-level optimization framework.

Despite these advances, all existing MTSF backdoor attacks, including **BackTime**, are limited to MSTSF settings with prediction horizons of at most 12 steps. Consequently, the vulnerability of MLTSF models to backdoor attacks remains entirely unexplored. Given MLTSF’s growing importance in critical sectors, addressing this research gap is urgent and essential. For example, in the energy sector, backdoor manipulation of long-term load forecasts could cause widespread blackouts or significant resource misalignment [14].

Nevertheless, extending backdoor attacks from MSTSF to MLTSF is challenging. The much longer input and output horizons in MLTSF exacerbate two key challenges: (i) In MLTSF, a local and stealthy trigger is expected to manipulate predictions hundreds of steps ahead. However, the model’s temporal dependencies rapidly attenuate such perturbations, making it difficult to design a trigger whose effect persists over long horizons. (ii) Under low poisoning rates, the poisoned window occupies only a tiny fraction of the thousands of

timesteps in MLTSF. This extreme sparsity causes the backdoor signal to be overwhelmed by clean sequences and hinders the model from learning a reliable trigger–target association.

In this paper, we propose a novel and effective backdoor attack on MLTSF, termed *BadTime*. By injecting a subtle trigger into multivariate historical inputs, *BadTime* can effectively induce the model to output an attacker-predefined target pattern over a long future horizon of 720 steps. Fig. 1 illustrates an attack example of the *BadTime*.

To address challenge (i), *BadTime* leverages the temporal dependencies and inter-variable correlations inherent in MLTSF data to design a trigger that remains effective across hundreds of future timesteps. This is achieved through three meticulous trigger designs: First, *BadTime* employs Graph Attention Networks (GATs) to model inter-variable influence [15], to select variables whose perturbations most strongly propagate to the target variables, and injects trigger fragments into them. Second, *BadTime* proposes a lag-aware positioning strategy that leverages temporal dependencies to insert the trigger at timestamps aligned with peak delayed correlation, ensuring activation precisely when its causal impact is maximal. Finally, *BadTime* constructs a puzzle-structured trigger and initializes it by extracting input segments that precede the best-matching target occurrence according to each variable’s optimal lag.

To address challenge (ii), *BadTime* enhances both the informativeness and learnability of poisoned samples to confront the extreme sparsity of backdoor signals. *BadTime* introduces a hybrid poisoned sample selection that encourages the model to treat the trigger as a higher-priority causal signal than the historical input, thereby enabling reliable learning of the trigger–target mapping despite the extreme scarcity of poisoned data. Moreover, *BadTime* decouples the backdoor training objectives from clean and poisoned samples, computing three separate terms: a clean loss, a backdoor loss on target variables of poisoned samples, and a fidelity loss on non-target variables of poisoned samples. This separation enables explicit up-weighting of the backdoor loss and adaptive focusing on scarce poisoned windows even under extremely low poisoning ratios. To ensure stealth, *BadTime* further incorporates a smoothness loss to penalize abrupt changes in the trigger and a range loss to constrain its values within historical min–max bounds.

Our main contributions are summarized as follows:

- **Problem.** We initiate the study of backdoor attacks in MLTSF and reveal severe, previously unexplored backdoor vulnerabilities in widely adopted MLTSF models.
- **Methodology.** We propose *BadTime*, a novel backdoor attack for MLTSF. To the best of our knowledge, *BadTime* is the first effective backdoor attack on MLTSF.
- **Evaluation.** Extensive experiments demonstrate that *BadTime* significantly outperforms the SOTA backdoor attack *BackTime* [13] on MSTSF. Specifically, *BadTime* extends the attackable horizon from at most 12 steps of *BackTime* to 720 steps (a 60× increase), and reduces its MAE on the target variable by over 50%. Moreover, *BadTime* achieves more than 3× higher stealth than *BackTime* under detection by USAD [16] and TranAD [17]. Finally, *BadTime* remains highly effective

TABLE I
DESCRIPTIONS AND DEFAULT SETTINGS OF KEY HYPERPARAMETERS AND NOTATIONS USED IN *BADTIME*

Symbol	Definition
α_P	Ratio of poisoned variables to total variables
α_S	The proportion of the V_i to the total number of variables
α_T	Ratio of poisoned samples in the training set
\mathcal{D}_c	The clean subsets of the training set \mathcal{D}
\mathcal{D}_p	The poisoned subsets of the training set \mathcal{D}
$\delta_{v_i}^*$	Optimal lag where trigger on v_i maximally influences V_i
γ	Ratio of poisoned samples whose ground-truth labels are most similar to p to the total number of poisoned samples
M	Epoch interval for trigger update
N	The number of variables
p	The target pattern
t_i	The timestamps
t_{IN}	The length of time windows
t_{OUT}	The prediction time steps
t_{PIN}	The length of target pattern p
t_{TGR}	Length of the full trigger across all poisoned variables
T	The time span
\mathcal{T}_{diff}	Indices of samples with labels most dissimilar to p
\mathcal{T}_{poison}	Indices of poisoned windows
\mathcal{T}_{sim}	Indices of samples with labels most similar to p
TGR_i	The trigger segment assigned to the i -th variable in V_p
τ	The trigger
θ	Parameters of the forecasting model being trained
λ	The proportion used for interpolating between the original input and the trigger during the trigger insertion process
μ	Ratio of target pattern length to output window length
ρ	Ratio of total trigger length to input window length
V_p	Set of variables into which trigger segments are injected
V_t	The set of variables manipulated toward p
X	The multivariate time series dataset

even with only 1% poisoned data and preserves strong forecasting performance on clean inputs.

The remainder of this paper is organized as follows. Section II discusses the fundamentals of MLTSF and provides a comprehensive review of existing backdoor attacks on time series models. Section III presents the threat model for our attack and provides a formal problem formulation. In Section IV, we introduce the proposed attack, *BadTime*, detailing its core mechanisms for data poisoning and backdoor training. Section V presents extensive experimental results to evaluate the effectiveness and stealthiness of the proposed method. Finally, Section VI concludes the paper.

II. RELATED WORK

In this section, we review the related works. Table I summarizes the notation used in this paper.

A. Multivariate Long-Term Series Forecasting

Multivariate Long-Term Time Series Forecasting (MLTSF) aims to predict long sequences (often 96, 192, 336, or even 720 time steps) of multiple values based on historical observations. Formally, a multivariate time series dataset is denoted as $X = \{x_1, x_2, \dots, x_N\} \in \mathbb{R}^{T \times N}$, where T is the time span, N is the number of variables, and each row records all variables at a given time. Training data are typically constructed via a sliding window: at each time point t_i , an input sequence of length t_{IN} is $X_{t_i} = X[t_i - t_{IN} : t_i]$, and the subsequent t_{OUT} steps are the ground-truth labels $Y_{t_i} = X[t_i + 1 : t_i + t_{OUT} + 1]$. Typically,

t_{IN} is set to 96 and $t_{OUT} \in \{96, 192, 336, 720\}$. The model is trained to predict the future sequence by minimizing a loss function between the predicted outputs and the corresponding targets. With its ability to capture long-term trends and complex dependencies among variables, MLTSF is widely used in energy management, traffic forecasting, financial analysis, and weather forecasting etc., and its prediction results often directly affect system scheduling, risk control, and strategic decisions.

B. Backdoor Attacks on Deep Time Series Models

Backdoor attacks typically inject the hidden behavior pattern into a model by poisoning a small portion of the training data. The model is then trained on the poisoned dataset using the following objective [11]:

$$\min_{\theta} \mathcal{L} = \mathbb{E}_{(x,y) \in \mathcal{D}_c} \ell(f_{\theta}(x), y) + \mathbb{E}_{(x',y_t) \in \mathcal{D}_p} \ell(f_{\theta}(x'), y_t), \quad (1)$$

where \mathcal{D}_c and \mathcal{D}_p denote the clean and poisoned subsets of the training set \mathcal{D} , respectively. The resulting backdoored model behaves normally on clean inputs but outputs an attacker-predefined target pattern when the trigger is present. Recently, an increasing number of studies has extended backdoor attacks to time series, particularly in time series classification task [18]–[20] and MSTSF task [12], [13].

1) *Backdoor attacks for time series classification:* BackTransfer [18] first introduced the concept of backdoor attacks into pre-trained time series classification models by embedding triangular waveform triggers and modifying labels, thereby enabling effective transferability to downstream tasks. Building on this, BPoET [19] targeted encrypted traffic classification, embedding handcrafted triggers via packet padding and refining them with a UAP-based strategy to improve stealth and effectiveness. Subsequent works explored more dynamic and adaptive trigger designs. For instance, TrojanFlow [20] jointly optimized a trigger generator and the target classifier to embed sample-specific dynamic triggers, while TimeTrojan [21] leveraged gradient saliency maps to select the most sensitive time steps for target class prediction as insertion positions, and further optimized trigger parameters with differential evolution algorithms. Along the same line, TimeGen [22] advanced the idea of stealthiness by generating sample-specific triggers via Generative Adversarial Networks.

More recently, research has also sought to reduce reliance on poisoned datasets and enhance stealth. TrojanTime [23] proposed a backdoor framework that avoids poisoning the training dataset by adversarial augmentation and logits alignment for pseudo-data-driven training, and ensuring invisibility through BatchNorm freezing and bidirectional loss. Meanwhile, FreqBack [24] exploited models’ varying sensitivity across frequency bands and used frequency-domain heatmaps to generate model-specific triggers in the frequency domain.

On the defensive side, E2ABL [25] introduced a unified framework that incorporates an auxiliary head to detect potential backdoors and correct poisoned labels, thus offering protection particularly against frequency-based attacks.

2) *Backdoor attacks for time series forecasting:* TAPTS [12] was the first to extend backdoor attacks to this domain, systematically defining the goal of backdoor attacks in time

TABLE II
COMPARISON OF BACKDOOR ATTACKS ON TIME SERIES. “N/A” INDICATES THAT THE METHOD IS NOT CAPABLE OF ATTACKING FORECASTING MODELS, AND THUS NO MANIPULATION LENGTH IS REPORTED.

Attack	Task	Manipulation length
BackTransfer [18]	Classification	N/A
BPoET [19]	Classification	N/A
TrojanFlow [20]	Classification	N/A
TimeTrojan [21]	Classification	N/A
TSBA [22]	Classification	N/A
TrojanTime [23]	Classification	N/A
FreqBack [24]	Classification	N/A
TAPTS [12]	Forecasting	7
BackTime [13]	Forecasting	12
BadTime (Ours)	Forecasting	720

series forecasting as outputting attacker-predefined values at specified time steps. BackTime [13] further advanced this line of work related to MTSF by leveraging graph convolutional networks to model variable dependencies and employing a bi-level optimization framework to train the target model and the trigger generator jointly.

Motivation. While backdoor attacks on time series have advanced in classification and short-term forecasting, as summarized in Table II, they remain entirely unexplored in multivariate long-term forecasting (MLTSF). Given MLTSF underpins strategic decision-making in critical domains such as energy and finance [26], this research gap presents a serious security vulnerability, motivating our work to develop the first effective backdoor attack framework for MLTSF.

III. THREAT MODEL AND PROBLEM FORMULATION

A. Threat Model of Backdoor Attacks on MLSTF

Capability of attackers: We consider a realistic threat model in which the adversary hosts a malicious third-party training platform. In this scenario, the victim uploads their raw time series data, model, and training configuration. The adversary thus can poison the training data and modify the training pipeline, but is restricted from altering the model architecture to avoid detection. Once deployed, the backdoored model can be activated by injecting a trigger into the input sequences. This threat model aligns with both practical outsourcing scenarios and recent work on time series backdoor attacks [13], [22].

Goals of attackers: (i) The backdoored model produces accurate forecasts aligned with the ground-truth labels when given clean inputs. (ii) When the input history contains the trigger τ , the model predicts the future of the target variables aligned with the given target pattern p .

B. Problem Formulation

Problem: Backdoor attacks on an MLTSF task.

Input: (i) A clean time series dataset $X \in \mathbb{R}^{T \times N}$. (ii) Target variable(s) V_t to be attacked (also call it attacked variable(s)). (iii) A predefined target pattern $p \in \mathbb{R}^{t_{PIN} \times |V_t|}$ with length t_{PIN} . (iv) Hyperparameters detailed in Appendix B.

Output: A backdoored forecasting model that predict the target pattern on V_t when poisoned inputs contain triggers, while maintaining normal performance on clean inputs.

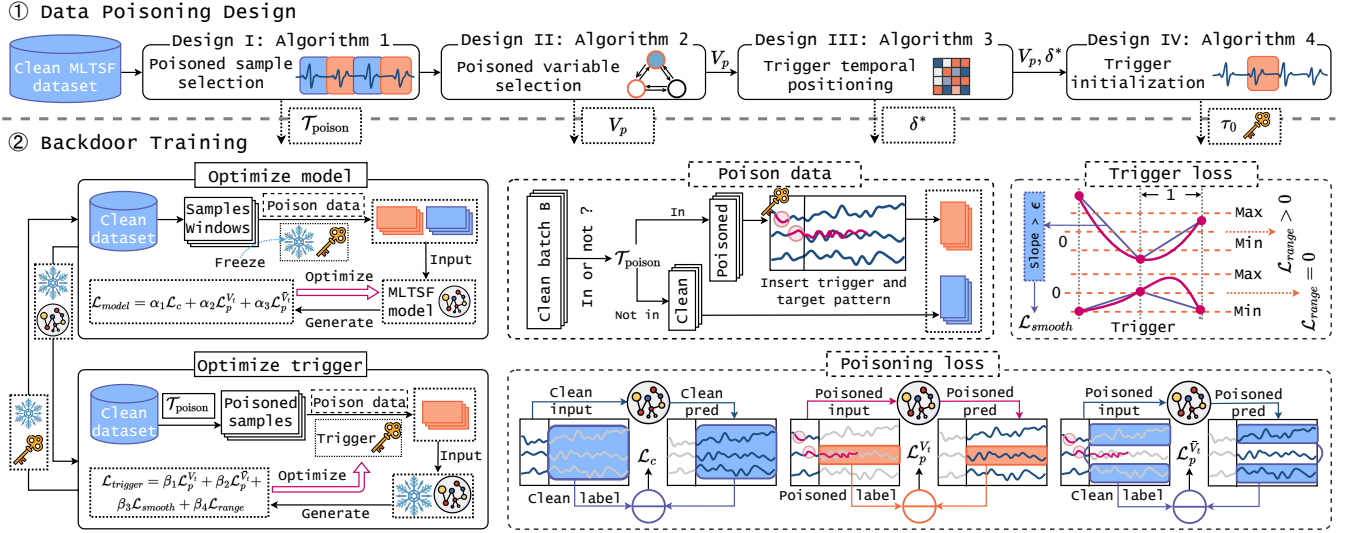


Fig. 2. Overview of the proposed BadTime attack. The top row shows four elaborate designs for data poisoning, and the bottom row depicts the backdoor training stage, where the introduced custom multi-objective loss functions are employed to optimize the model and trigger alternately.

IV. PROPOSED METHOD: BADTIME

In this section, we introduce the proposed backdoor attack BadTime for MLTSF models.

A. Overall Workflow

As illustrated in Fig. 2, BadTime comprises two phases: **data poisoning design** and **backdoor training**. In the data poisoning design phase, we specify which samples and variables to poison, when to insert triggers, and how to construct the trigger. In the subsequent backdoor training phase, we introduce a series of optimization objectives tailored to the sparse and temporal nature of MLTSF data. Based on this objective, we apply the poisoning designs from the first phase to poison the data and use this poisoned data to perform an alternating optimization between the model and the trigger.

B. Poisoned Data Design

In this subsection, we detail four carefully crafted designs that constitute the poisoning strategy:

- Design I: Which samples to poison?
- Design II: Which variables to perturb?
- Design III: Where in time to insert triggers?
- Design IV: What trigger to use?

Design I: Which samples to poison?

Selecting which training samples to poison is a critical step in backdoor injection. Existing work [13] selects samples whose model predictions are closest to the target pattern. While intuitive, this approach heavily relies on the accuracy of model predictions, thus requiring thorough pretraining on clean data, which incurs substantial computational cost.

To overcome these limitations, we propose a hybrid selection strategy that leverages the similarity between ground-truth

labels and the target pattern to identify a subset of training samples for poisoning, while leaving the rest of the dataset intact. The overall procedure is outlined in Algorithm 1. Specifically, we select two types of samples for poisoning: (i) samples whose ground-truth labels $X_{t_i:t_i+t_{OUT}}^{V_t}$ are most similar to the target pattern (label-similar samples) and (ii) those whose labels most differ from the target pattern (label-dissimilar samples).

Algorithm 1 Select poisoned sample

Input: An MLTSF dataset $X \in \mathbb{R}^{T \times N}$, target pattern $p \in \mathbb{R}^{t_{PIN}}$, temporal poisoning ratio α_T , similarity proportion ρ , target pattern coverage ratio μ
Output: Poisoned timestamp indices \mathcal{T}_{poison}

- 1: $t_{PIN} \leftarrow \mu \cdot t_{OUT}$ \triangleright Target pattern length
- 2: Initialize an empty distance map $D[\cdot]$
- 3: **for** each training window with start timestamp $t_i - t_{IN}$ in \mathcal{D}_{train} **do**
- 4: $y_i \leftarrow X_{t_i:t_i+t_{PIN}}^{V_t}$ \triangleright Ground-truth label segment on V_t
- 5: $D[t_i] \leftarrow \|y_i - p\|_2$ \triangleright Euclidean distance
- 6: **end for**
- 7: $k_{sim} \leftarrow \lfloor \gamma \cdot \alpha_T \cdot |\mathcal{D}_{train}| \rfloor$
- 8: $k_{diff} \leftarrow \lfloor (1 - \gamma) \cdot \alpha_T \cdot |\mathcal{D}_{train}| \rfloor$
- 9: $\mathcal{T}_{sim} \leftarrow \text{TopK}_{t_i}(-D[t_i], k_{sim})$ \triangleright Most similar
- 10: $\mathcal{T}_{diff} \leftarrow \text{TopK}_{t_i}(D[t_i], k_{diff})$ \triangleright Most dissimilar
- 11: $\mathcal{T}_{poison} \leftarrow \mathcal{T}_{sim} \cup \mathcal{T}_{diff}$
- 12: **return** \mathcal{T}_{poison}

In this selection, label-similar samples, whose ground-truths already resemble the target pattern, naturally produce outputs close to it. Consequently, they require only a subtle trigger to steer the output, enhancing attack stealthiness. By contrast, label-dissimilar samples naturally suppress the target pattern. When triggered and relabeled, these samples create a conflict: the original features oppose the new target supervision. To resolve this, the model learns the trigger as a high-priority

shortcut that overrides the input, thereby strengthening attack effectiveness and robustness.

We formalize our poisoned sample selection as follows. Let $\mathcal{T}_{poison} = \{t_1, t_2, \dots, t_k\}$ denote the set of start timestamps of poisoned label windows. Our hybrid selection is defined as:

$$\begin{cases} \mathcal{T}_{poison} = \mathcal{T}_{sim} + \mathcal{T}_{diff} \\ \mathcal{T}_{sim} = \text{TopK}_{t_i}(-d(t_i), k = \gamma \cdot \alpha_T \cdot |\mathcal{D}_{train}|) \\ \mathcal{T}_{diff} = \text{TopK}_{t_i}(d(t_i), k = (1 - \gamma) \cdot \alpha_T \cdot |\mathcal{D}_{train}|) \end{cases}, \quad (2)$$

where \mathcal{T}_{sim} denotes the set of timestamps indices for samples with labels most similar to the target pattern, \mathcal{T}_{diff} denotes the set of timestamps indices for samples with labels most different to the target pattern, α_T denotes the poisoning ratio, $\gamma \in (0, 1)$ controls the ratio between the two sample types, and the $d(t_i)$ is the distance between the label of the sample with start timestamp $t_i - t_{IN}$ on V_t and the target pattern p , where we use the Euclidean distance as the similarity metric:

$$d(t_i) = \left\| X_{t_i:t_i+t_{PIN}}^{V_t} - p \right\|_2. \quad (3)$$

Observation 1: We find that poisoning only one of the two sample types fails to achieve optimal attack performance, as confirmed by our ablation study in Table VII. This is because each type has systematic input features (either encouraging or discouraging the target). When only one type is used, the model attributes the target pattern to these input-specific features rather than the trigger, resulting in a weak and context-dependent trigger-target association.

Design II: Which variables to poison?

We define the poisoned variables V_p as the part input variables into which the trigger is embedded to induce predictions on the target variables V_t . Prior works [13], [27] set $V_p = V_t$, i.e., injecting the trigger directly into the target variables. This choice increases trigger exposure risk for two reasons: (i) abnormal outputs on the target variable naturally prompt scrutiny of its inputs; (ii) concentrating the entire trigger in a single variable yields longer, more conspicuous perturbations.

We leverage the inherent inter-variable dependencies in multivariate time series to mitigate this. We observe that advanced MLTSF models [8], [9], [28]–[30] tend to use inter-variable correlations to enhance their forecasting performances. This means the prediction of the target variable V_t is influenced by its closely correlated variables. Based on this observation, we distribute the trigger across multiple variables that are closely correlated to the target variable V_t rather than embedding it solely in V_t . Specifically, we train a lightweight GAT to learn predictive dependencies, score each variable by its total contribution to predicting V_t , and select the top $\alpha_p \cdot |V|$ as V_p . The trigger is then split into $|V_p|$ equal fragments and embedded into these variables. This procedure is visualised in Fig. 3 and summarized in Algorithm 2.

Given a multivariate time series $X = \{x_1, x_2, \dots, x_N\} \in \mathbb{R}^{T \times N}$, we represent each variable as a node in a fully connected directed graph $G = (V, E)$. The feature of node

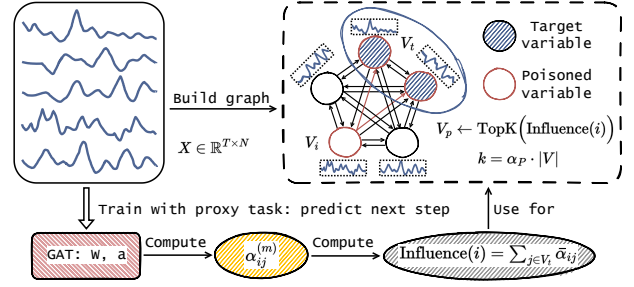


Fig. 3. Workflow of our poisoned variable selection. From the multivariate series X , we build a directed graph and train a GAT with a proxy task of predicting next step on V_t to obtain edge attentions. Averaged attentions α_{ij} are aggregated as $\text{Influence}(i) = \sum_{j \in V_t} \bar{\alpha}_{ij}$, and the top- k variables by this score are selected as V_p .

Algorithm 2 Poisoned variable selection

Input: An MLTSF dataset $X \in \mathbb{R}^{T \times N}$, target set V_t , ratio α_p , heads n_{head}
Output: V_p

- 1: $H \in \mathbb{R}^{N \times T} \leftarrow$ standardize X
- 2: $h_i \leftarrow H[i, :]$
- 3: $V \leftarrow \{1, \dots, N\}$
- 4: $E \leftarrow V \times V$
- 5: $G \leftarrow (V, E)$
- 6: Train a GAT with n_{head} heads on $H \in \mathbb{R}^{N \times T}$ to predict next step on V_t
- 7: Compute $\alpha_{ij}^{(m)}$ for all $(i \rightarrow j) \in E$ and $m = 1, \dots, n_{head}$ as Eq. 4
- 8: $\bar{A}[i, j] \leftarrow \bar{\alpha}_{ij} \leftarrow \frac{1}{n_{head}} \sum_{m=1}^{n_{head}} \alpha_{ij}^{(m)}$
- 9: **for** each $i \in V$ **do**
- 10: $\text{Influence}(i) \leftarrow \sum_{j \in V_t} \bar{A}[i, j]$
- 11: **end for**
- 12: $V_p \leftarrow \text{TopK}(\text{Influence}(i), k = \alpha_p \cdot |V|)$
- 13: **return** V_p

i is a standardized time series $h_i = H[i, :] \in \mathbb{R}^T$, where $H \in \mathbb{R}^{N \times T}$ is constructed by z-scoring each variable over the training horizon. To capture predictive dependencies among variables, we train a lightweight GAT with only one single layer on a next-step prediction proxy task focused on the target variables. This proxy training is much faster than pretraining the forecasting model to convergence as in the SOTA work [13]. After training, we compute attention on each directed edge $i \rightarrow j$. For head $m \in 1, \dots, n_{head}$ with $n_{head} = 4$:

$$\alpha_{ij}^{(m)} = \frac{\exp(\text{LeakyReLU}((a^{(m)})^T [W^{(m)} h_i \parallel W^{(m)} h_j]))}{\sum_{k \in \mathcal{N}_j} \exp(\text{LeakyReLU}((a^{(m)})^T [W^{(m)} h_k \parallel W^{(m)} h_j]))}, \quad (4)$$

where $W^{(m)}$ and $a^{(m)}$ are learnable parameters by training GAT, h_i is the feature of node i , \parallel denotes vector concatenation, and \mathcal{N}_j is the set of incoming neighbors of node j and includes i itself. We average $\alpha_{ij}^{(m)}$ over all heads to obtain $\bar{\alpha}_{ij} \in [0, 1]$. In the trained GAT, node j computes its representation through a softmax-normalized aggregation over its incoming neighbors, and $\bar{\alpha}_{ij}$ reflects the proportion of information from node i used to predict j . Since the GAT is trained to minimize the proxy loss on the target variables V_t , higher attention weights are

assigned to neighbors that provide stronger predictive signals. Thus, $\bar{\alpha}_{ij}$ serves as a measure of the predictive contribution of variable i to variable j . We then compute a cumulative influence score for each variable i by summing its attention weights toward all target variables:

$$\text{Influence}(i) = \sum_{j \in V_t} \bar{\alpha}_{ij}. \quad (5)$$

Based on the influence scores, we select the top $\alpha_p \cdot |V|$ variables as the poisoned set V_p .

Observation 2: Selected poisoned variables V_p typically include the target variables, since each target variable exerts a stronger influence on its own prediction than any other variable.

Design III: *Where in timestamps to insert triggers?*

After selecting the poisoned variables, we therefore identify effective timestamps for trigger injection on these variables. In time series, strong temporal dependencies and delayed effects make injection time far more critical than spatial trigger placement in images, yet most existing methods ignore this temporal aspect. For example, BackTime [13] inserts the trigger by overwriting the last t_{TGR} time steps of the target variable, based on the intuition that inputs closer to the forecast horizon exert the strongest influence on predictions. This heuristic lacks a data-driven justification, offers limited interpretability and overlooks that predictive influence between variables is often delayed rather than immediate. For instance, temperature can affect electricity demand several hours later, and changes in heart rate can precede changes in blood pressure. Consequently, a fixed, horizon-adjacent trigger placement may miss the true causal or predictive lags in the data.

To address this, we propose a lag-aware positioning strategy that estimates. The complete procedure is summarized in Algorithm 3. For each poisoned variable $v_i \in V_p$, we estimate an optimal lag $\delta_{v_i}^*$ that specifies how many steps in advance the trigger should be inserted to most effectively influence predictions on the target variables V_t . The trigger fragment for v_i is placed $\delta_{v_i}^*$ steps before the target pattern's onset to ensure it takes effect precisely when the model predicts the target output. Specifically, for each poisoned variable $v_i \in V_p$, we determine its optimal lag $\delta_{v_i}^*$ as follows:

$$\delta_{v_i}^* = \arg \max_{\delta \in [\frac{t_{TGR}}{|V_p|}, t_{IN}]} \sum_{v_j \in V_t} \sum_{t=0}^{|X|-t_{IN}} \text{Corr}(X^{v_i}[t : t + t_{IN} - \delta], X^{v_j}[t + \delta : t + t_{IN}]), \quad (6)$$

where the function $\text{Corr}(X^{v_i}, X^{v_j})$ calculates Pearson correlation coefficient [31], which is calculated as:

$$\text{Corr}(X^{v_i}, X^{v_j}) = \frac{\text{Cov}(X^{v_i}, X^{v_j})}{\sigma_{v_i} \sigma_{v_j}}, \quad (7)$$

where $\text{Cov}(x, y)$ is the covariance between x and y , and σ_x, σ_y are their standard deviations, respectively. For each candidate lag δ , the objective in Eq. 6 computes the Pearson correlation between the prefix of v_i and the δ -shifted suffix of each

target variable v_j within every input window, then aggregates these correlations across all windows and target variables. The optimal lag $\delta_{v_i}^*$ is the one that maximizes this aggregated score, indicating that v_i exhibits the strongest and most consistent association with the targets when leading them by δ steps.

Let $\delta^* = [\delta_1^*, \delta_2^*, \dots, \delta_{|V_p|}^*]$ denote the optimal lags for all poisoned variables. For a poisoned sample starting at time t , the trigger fragment for variable v_i is inserted at the interval $[t + t_{IN} - \delta_{v_i}^* : t + t_{IN} - \delta_{v_i}^* + \frac{t_{TGR}}{|V_p|}]$. The full trigger is evenly segmented and injected into the poisoned variables according to their respective lags.

Algorithm 3 Trigger temporal positioning

Input: An MLTSF dataset $X \in \mathbb{R}^{T \times N}$, poisoned variables V_p , target variables V_t , input length t_{IN} , total trigger length t_{TGR}

Output: $\delta^* = [\delta_{v_1}^*, \dots, \delta_{v_{|V_p|}}^*]$

```

1:  $L \leftarrow \lceil t_{TGR}/|V_p| \rceil$  ▷ minimum feasible lag
2: for each  $v_i \in V_p$  do
3:   for  $\delta = L$  to  $t_{IN}$  do
4:      $C_{v_i}[\delta] \leftarrow 0$ 
5:     for  $t = 0$  to  $T - t_{IN}$  do
6:       for each  $v_j \in V_t$  do
7:          $C_{v_i}[\delta] += \text{Corr}(X^{v_i}[t : t + t_{IN} - \delta], X^{v_j}[t + \delta : t + t_{IN}])$ 
8:       end for
9:     end for
10:  end for
11:   $\delta_{v_i}^* \leftarrow \arg \max_{\delta \in [L, t_{IN}]} C_{v_i}[\delta]$ 
12: end for
13: return  $\delta^*$ 

```

Design IV: *What trigger to use?*

To accelerate convergence of both the model and the trigger in subsequent optimization, we construct an effective initial trigger using a data-driven strategy. This strategy selects in-distribution temporal fragments that the model already tends to map to the target pattern under its priors, thereby positioning the optimization closer to a feasible solution. Specifically, we extract trigger values from training samples whose ground-truth labels most closely match the target pattern p . The time index t^* is selected by minimizing the Euclidean distance between the label segment and p as follows:

$$t^* = \arg \min_t \|X_{t:t+t_{PIN}} - p\|_2. \quad (8)$$

For each poisoned variable $v_i \in V_p$, we extract a segment of length $t_{TGR}/|V_p|$ by backtracking from t^* according to its optimal lag $\delta_{v_i}^*$:

$$\text{TGR}_i = X_{t^* - \delta_{v_i}^* : t^* - \delta_{v_i}^* + t_{TGR}/|V_p|}. \quad (9)$$

The initial trigger matrix τ_0 is then formed by concatenating all trigger segments:

$$\tau_0 = [\text{TGR}_1, \text{TGR}_2, \dots, \text{TGR}_{|V_p|}]. \quad (10)$$

The full procedure is detailed in Algorithm 4.

Algorithm 4 Initialize trigger

Input: An MLTSF dataset $X \in \mathbb{R}^{T \times N}$, poisoned variable set V_p , target pattern p , optimal lags δ^* , target pattern length t_{PIN} , total trigger length t_{TGR}

Output: Initial trigger matrix τ_0

- 1: $t^* \leftarrow \arg \min_t \|X_{t:t+t_{PIN}} - p\|_2$ ▷ Locate best-matching subsequence
- 2: Initialize empty trigger matrix τ_0
- 3: **for** each poisoned variable $v_i \in V_p$ with lag $\delta_{v_i}^*$ **do**
- 4: Extract trigger segment:

$$\text{TGR}_i \leftarrow X^{v_i} \left[t^* - \delta_{v_i}^* : t^* - \delta_{v_i}^* + \frac{t_{TGR}}{|V_p|} \right]$$

- 5: Append TGR_i to τ_0
- 6: **end for**
- 7: **return** $\tau_0 = [\text{TGR}_1, \text{TGR}_2, \dots, \text{TGR}_{|V_p|}]$

C. Backdoor Training

Using the four data poisoning designs from Phase I, we now embed the backdoor into the MLTSF model. Specifically, the clean training dataset X is dynamically poisoned during training according to the its poisoned configuration designed from Phase I: samples indexed by \mathcal{T}_{poison} (Design I) are selected to poison, triggers are injected into selected poisoned variables V_p (Design II) at lags δ^* (Design III), and the initial trigger τ_0 (Design IV) seeds the optimization. This poisoned data is then used to train the model and the trigger via alternating optimization, as detailed in the following subsections. Throughout the whole optimization, \mathcal{T}_{poison} , V_p , and δ^* remain fixed, and only the trigger is updated.

Observation 3: Alternating optimization of the model and the trigger is not a new technique and is widely used in existing backdoor attacks [32]–[34]. However, directly applying this technique to MLTSF leads to attack failure because stealth constraints yield extremely sparse backdoor signals. Under such sparsity, conventional losses are dominated by clean data and clean segments in poisoned samples, causing the model to overlook the trigger–target correlation. Our ablation study (w/o-CustomObj, Table VII) confirms that this leads to complete attack failure. To overcome sparsity of backdoor signals in MLTSF, we keep the alternating optimization framework but design a series of **custom loss objectives tailored to MLTSF task**.

1) *Model optimization step:* At model optimization iteration m , we fix the current trigger τ_k and optimize the model parameters θ . When $k = 0$, τ_k is initialized as trigger τ_0 precomputed in Design IV.

Let the current iteration batch be denoted as $B = \{(X_i, Y_i, t_i)\}$, where t_i denotes the start timestamp of sample i , we partition B into poisoned and clean subsets using the precomputed timestamp set \mathcal{T}_{poison} :

$$B_p = \{(X_i, Y_i, t_i) \in B \mid t_i \in \mathcal{T}_{poison}\}, \quad B_c = B \setminus B_p. \quad (11)$$

For each $(X_i, Y_i, t_i) \in B_p$ and each poisoned variable $v_j \in V_p$, we inject the j -th fragment of τ_k into the interval:

$$\mathcal{I}_j = \left[t_{IN} - \delta_{v_j}^* : t_{IN} - \delta_{v_j}^* + \frac{t_{TGR}}{|V_p|} \right] \quad (12)$$

via linear interpolation:

$$X_i^{v_j}[\mathcal{I}_j] = (1 - \lambda) X_i^{v_j}[\mathcal{I}_j] + \lambda \tau_k[j], \quad (13)$$

where $\lambda \in [0, 1]$ controls the blend between the original input and the trigger, enhancing stealth by preserving part of the original sequence.

Next, we modify the ground-truth label Y_i as follows. For the target variables V_t , the first $t_{PIN} = \mu \cdot t_{OUT}$ timesteps are replaced with the target pattern p , while the remaining timesteps and all non-target variables remain unchanged:

$$\tilde{Y}_i^v = \begin{cases} p, & v \in V_t \text{ at } [0 : t_{PIN}] \text{ timesteps} \\ Y_i^v, & \text{otherwise} \end{cases}, \quad (14)$$

where t_{PIN} denotes the length of the target pattern and μ denotes its proportion within the output window. Samples in B_c are left unmodified.

Then, the batch B containing the poisoned subset B_p and clean subset B_c are fed into the target MLTSF model $f(\theta)$ to obtain predictions $\hat{Y}_i = f(B, \theta)$, and the total loss is computed using our proposed objective:

$$\mathcal{L}_{model} = \alpha_1 \mathcal{L}_c + \alpha_2 \mathcal{L}_p^{V_t} + \alpha_3 \mathcal{L}_p^{\tilde{V}_t}, \quad (15)$$

where α_1 , α_2 and α_3 are weights for the three loss terms and they are set based on experimental experience. Fig. 2 provides a visual walkthrough of how these three loss components are computed. The clean loss \mathcal{L}_c is computed over clean samples and ensures that the model maintains its performance on the primary forecasting task:

$$\mathcal{L}_c = \frac{1}{|B_c|} \sum_{i \in B_c} \left(\|\hat{Y}_i - Y_i\|_2^2 + \|\hat{Y}_i - Y_i\|_1 \right), \quad (16)$$

$\mathcal{L}_p^{V_t}$ is the loss computed on target variables of poisoned samples, enabling the model to learn the mapping between the trigger and target pattern:

$$\mathcal{L}_p^{V_t} = \frac{1}{|B_p|} \sum_{i \in B_p} \left(\|\hat{Y}_{i, V_t} - \tilde{Y}_i^{V_t}\|_2^2 + \|\hat{Y}_{i, V_t} - \tilde{Y}_i^{V_t}\|_1 \right), \quad (17)$$

where \tilde{Y} denotes poisoned labels with the target pattern. $\mathcal{L}_p^{\tilde{V}_t}$ constrains predictions on non-target variables of poisoned samples to match their clean ground-truths, counteracting potential side effects caused by trigger injection into non-target (but poisoned, i.e., $V_p \setminus V_t$) variables and ensuring the attack only affects the target variables:

$$\mathcal{L}_p^{\tilde{V}_t} = \frac{1}{|B_p|} \sum_{i \in B_p} \left(\|\hat{Y}_i^{\tilde{V}_t} - Y_i^{\tilde{V}_t}\|_2^2 + \|\hat{Y}_i^{\tilde{V}_t} - Y_i^{\tilde{V}_t}\|_1 \right). \quad (18)$$

Although the three terms share a similar form, we keep the three loss terms separate rather than merging them into a single objective to address the extreme sparsity of backdoor signals in MLTSF under low poisoning ratios. When losses are combined, the overwhelming dominance of clean data causes the model to ignore the trigger–target association in the few poisoned samples, leading to attack failure. Separating the losses enables

explicit upweighting of $\mathcal{L}_p^{V_t}$ and adaptively tunes the weights of all terms according to poisoning settings, such as poisoning ratios, trigger length, and target pattern length and so on. This adaptive weighting strategy is crucial for mitigating the sparsity of backdoor signals in MLTSF and ensuring attack success.

Finally, model parameters are then updated via:

$$\theta^{m+1} = \theta^m - \eta \cdot \nabla_{\theta^m} \mathcal{L}_{model}. \quad (19)$$

2) *Trigger optimization step*: Every M epochs, we freeze the model parameters and update the current trigger τ_k to adapt it to the evolving model. We iterate over poisoned samples from the training set using the precomputed timestamp set \mathcal{T}_{poison} , embed triggers into them, replace ground-truth labels with the target pattern, as described in the model update step above, after which the poisoned data is fed into the model and the trigger updated by minimizing the loss function:

$$\mathcal{L}_{trigger} = \beta_1 \mathcal{L}_p^{V_t} + \beta_2 \mathcal{L}_p^{\bar{V}_t} + \beta_3 \mathcal{L}_{smooth} + \beta_4 \mathcal{L}_{range}, \quad (20)$$

where $\mathcal{L}_p^{V_t}$ and $\mathcal{L}_p^{\bar{V}_t}$ are identical to those in model optimization. Fig. 2 provides a visualization of the computation of \mathcal{L}_{smooth} and \mathcal{L}_{range} . The smoothness loss \mathcal{L}_{smooth} penalizes abrupt changes in trigger values to enhance temporal continuity:

$$\mathcal{L}_{smooth} = \frac{1}{t_{TGR}} \sum_{i=1}^{t_{TGR}/|V_p|} \sum_{j=1}^{|V_p|} [\max(|\tau_k^i[j] - \tau_k^{i-1}[j]| - \varepsilon, 0)]^2, \quad (21)$$

where ε is the smoothness threshold, set to 0.8 empirically. The range loss \mathcal{L}_{range} constrains each trigger value within the min–max range of its corresponding poisoned variable:

$$\mathcal{L}_{range} = \frac{1}{t_{TGR}} \sum_{i=1}^{|V_p| t_{TGR}/|V_p|} \sum_{j=1}^{|V_p|} \left[\max\left(\min(X^{v_i}) - \tau_k^j[i], 0\right) + \max\left(\tau_k^j[i] - \max(X^{v_i}), 0\right) \right], \quad (22)$$

V. EXPERIMENTS

A. Experimental Setup

Datasets. We conduct experiments on seven widely adopted benchmark datasets in the MLTSF domain: ETTh1 [9], ETTh2 [9], ETTm1 [9], ETTm2 [9], Electricity [8], Weather [8], and Exchange [8]. These datasets cover various real-world scenarios, including power load, meteorological trends, and currency exchange rate fluctuations. Detailed descriptions of the datasets are provided in Appendix A.

Models. We select six mainstream MLTSF models as attack targets: Autoformer [8], Mamba [35], TimesNet [29], iTransformer [10], TSMixer [36], and TimeMixer [37]. These models cover four classic MLTSF backbone architectures: MLP-based, RNN-based, CNN-based, and Transformer-based, and are widely adopted as baselines in recent MLTSF research.

Metrics. We use Mean Absolute Error (MAE) [38] to evaluate forecasting performance and attack effectiveness. Specifically: (i) MAE_c measures the model’s clean forecasting performance by comparing predictions with ground-truth labels under clean inputs; (ii) MAE_{pa} assesses attack effectiveness by comparing predictions with the target pattern on target variables under trigger-embedded inputs; (iii) MAE_{pn} assesses side effects on non-target variables by comparing predictions with their clean label on non-target variables under trigger-embedded inputs. All the above metrics are better with smaller values.

TABLE III
DESCRIPTORS AND DEFAULT SETTINGS OF KEY HYPERPARAMETERS AND NOTATIONS USED IN BADTIME

Name	Symbol	Default value in experiments
Input length	t_{IN}	96
Label length	t_{OUT}	96
Target pattern length	t_{PIN}	53
Trigger length ratio	ρ	0.3
Temporal injection rate	α_T	0.1
Similarity mixing ratio	γ	0.3
Poison injection rate	α_P	0.3
Total trigger length	t_{TGR}	29
Interpolation weight	λ	1
Epoch interval for trigger update	M	2
Spatial injection rate	α_S	0.1
Target pattern coverage ratio	μ	0.55
Target pattern shape	-	Hump

Experiment protocol. We adopt model architectures and training hyperparameters from the Time Series Library (TSLib) ¹, a widely used benchmark. Unless otherwise stated, all experiments predict the next 96 timesteps using the previous 96 timesteps as input, with all other hyperparameters set to the defaults in Table III. In the main results, we compare BadTime against two baselines: Benign, which refers to models trained on clean data, and BackTime [13], the current SOTA backdoor attack for MTSF. **We evaluate against only one attack method because, to the best of our knowledge, BackTime is the only backdoor attack specifically designed for MTSF. Existing backdoor methods from other domains are not directly applicable without substantial modifications to both the attack strategy and threat model, which would compromise the fairness and relevance of the comparison.**

B. Main Results

1) *Effectiveness comparison*: We compare the performance of Benign, BackTime, and BadTime on six mainstream models and seven benchmark datasets. Table IV shows the experimental results. Firstly, considering the attack effectiveness, BadTime achieves the lowest average MAE_{pa} across all datasets and MLTSF models. Meanwhile, BadTime maintains competitive MLTSF capabilities. Finally, the MAE_{pn} of BadTime is almost equal to that of Benign, indicating that the triggers of BadTime have almost no side effects on the forecasting of non-target variables, owing to BadTime’s careful design of the triggers and their insertion locations. Fig. 4 provides a visual attack case of BackTime and BadTime on the same time series window from the ETTh1 dataset with the red curve denoting embedded triggers and target patterns. For clarity, only the target variable is shown. As illustrated, BadTime achieves stronger attack effectiveness by producing poisoned predictions that better match the target pattern than those of BackTime. Additionally, the trigger of BadTime is shorter, smoother, and more natural than that of BackTime. Moreover, BadTime better preserves forecasting performance on clean inputs, with predictions more closely aligned with ground-truth labels compared to BackTime.

¹<https://github.com/thuml/Time-Series-Library>

TABLE IV
COMPARISON OF FORECASTING ABILITY AND ATTACK PERFORMANCE ACROSS DATASETS AND MODELS. THE LOWER THE BETTER FOR ALL METRICS.
BOLD INDICATES THE BEST PERFORMANCE FOR THAT COLUMN.

Method	Datasets	Metric	Autoformer	Mamba	TimesNet	iTransformer	TSMixer	TimeMixer	Average
Benign	ETTh1	MAE _c	0.439	0.445	0.424	0.411	0.503	0.393	0.436
		MAE _{pa}	0.801	0.782	0.781	0.776	1.009	0.768	0.820
		MAE _{pn}	0.444	0.455	0.432	0.421	0.507	0.401	0.443
	ETTh2	MAE _c	0.395	0.372	0.374	0.349	0.874	0.342	0.451
		MAE _{pa}	0.782	0.790	0.793	0.784	0.961	0.792	0.817
		MAE _{pn}	0.409	0.385	0.387	0.362	0.956	0.354	0.476
	ETTh2	MAE _c	0.508	0.386	0.376	0.367	0.445	0.366	0.408
		MAE _{pa}	0.796	0.779	0.777	0.793	0.885	0.782	0.802
		MAE _{pn}	0.535	0.396	0.387	0.379	0.460	0.378	0.423
	ETTh2	MAE _c	0.295	0.275	0.268	0.274	0.479	0.261	0.309
		MAE _{pa}	0.512	0.516	0.517	0.517	0.522	0.515	0.517
		MAE _{pn}	0.306	0.283	0.276	0.280	0.475	0.267	0.315
	Electricity	MAE _c	0.323	0.317	0.285	0.245	0.312	0.253	0.289
		MAE _{pa}	0.854	0.761	0.732	0.725	0.814	0.718	0.767
		MAE _{pn}	0.347	0.342	0.305	0.288	0.359	0.283	0.321
	Weather	MAE _c	0.364	0.252	0.245	0.227	0.256	0.210	0.259
		MAE _{pa}	0.827	0.799	0.795	0.778	0.816	0.791	0.801
		MAE _{pn}	0.364	0.252	0.245	0.227	0.256	0.209	0.259
	Exchange	MAE _c	0.325	0.271	0.239	0.221	0.334	0.202	0.265
		MAE _{pa}	0.634	0.544	0.531	0.542	0.507	0.537	0.549
		MAE _{pn}	0.352	0.299	0.261	0.242	0.362	0.222	0.290
BackTime [13]	ETTh1	MAE _c	0.565	0.456	0.448	0.406	0.478	0.417	0.462
		MAE _{pa}	0.817	0.776	0.750	0.769	0.547	0.641	0.717
		MAE _{pn}	0.522	0.460	0.439	0.415	0.480	0.415	0.455
	ETTh2	MAE _c	0.456	0.397	0.380	0.352	1.021	0.363	0.495
		MAE _{pa}	0.763	0.811	0.792	0.758	0.717	0.694	0.756
		MAE _{pn}	0.454	0.410	0.384	0.365	1.136	0.370	0.520
	ETTh2	MAE _c	0.482	0.414	0.381	0.366	0.448	0.373	0.411
		MAE _{pa}	0.881	0.781	0.819	0.801	0.736	0.484	0.750
		MAE _{pn}	0.458	0.421	0.388	0.376	0.449	0.366	0.410
	ETTh2	MAE _c	0.347	0.278	0.269	0.266	0.418	0.262	0.307
		MAE _{pa}	0.643	0.532	0.526	0.552	0.464	0.537	0.542
		MAE _{pn}	0.338	0.283	0.274	0.273	0.420	0.265	0.309
	ETTh2	MAE _c	0.347	0.336	0.305	0.268	0.339	0.271	0.311
		MAE _{pa}	0.875	0.753	0.764	0.711	0.738	0.627	0.745
		MAE _{pn}	0.353	0.361	0.299	0.346	0.366	0.295	0.337
	ETTh2	MAE _c	0.325	0.246	0.221	0.213	0.240	0.210	0.243
		MAE _{pa}	0.800	0.777	0.726	0.724	0.596	0.535	0.693
		MAE _{pn}	0.324	0.242	0.216	0.213	0.233	0.206	0.239
	ETTh2	MAE _c	0.287	0.263	0.233	0.204	0.401	0.213	0.267
		MAE _{pa}	0.540	0.543	0.558	0.505	0.463	0.440	0.508
		MAE _{pn}	0.316	0.290	0.254	0.223	0.396	0.233	0.285
BadTime (Ours)	ETTh1	MAE _c	0.465	0.477	0.421	0.406	0.509	0.413	0.449
		MAE _{pa}	0.485	0.478	0.376	0.234	0.372	0.255	0.367
		MAE _{pn}	0.460	0.459	0.429	0.414	0.526	0.415	0.451
	ETTh2	MAE _c	0.417	0.406	0.361	0.366	0.769	0.363	0.447
		MAE _{pa}	0.412	0.391	0.329	0.216	0.617	0.274	0.373
		MAE _{pn}	0.442	0.428	0.355	0.379	0.886	0.377	0.478
	ETTh2	MAE _c	0.525	0.386	0.384	0.356	0.492	0.373	0.419
		MAE _{pa}	0.501	0.399	0.355	0.186	0.192	0.372	0.334
		MAE _{pn}	0.532	0.395	0.393	0.379	0.505	0.388	0.432
	ETTh2	MAE _c	0.297	0.281	0.267	0.261	0.374	0.266	0.291
		MAE _{pa}	0.315	0.281	0.223	0.203	0.324	0.169	0.253
		MAE _{pn}	0.322	0.306	0.271	0.284	0.430	0.274	0.315
	ETTh2	MAE _c	0.335	0.324	0.298	0.283	0.322	0.249	0.302
		MAE _{pa}	0.344	0.317	0.206	0.168	0.276	0.239	0.258
		MAE _{pn}	0.330	0.325	0.299	0.291	0.344	0.275	0.311
	ETTh2	MAE _c	0.389	0.245	0.233	0.225	0.238	0.212	0.257
		MAE _{pa}	0.447	0.231	0.202	0.209	0.172	0.179	0.240
		MAE _{pn}	0.382	0.242	0.238	0.224	0.231	0.213	0.255
	ETTh2	MAE _c	0.298	0.286	0.238	0.218	0.347	0.211	0.266
		MAE _{pa}	0.293	0.228	0.204	0.106	0.175	0.169	0.196
		MAE _{pn}	0.329	0.326	0.245	0.278	0.411	0.249	0.306

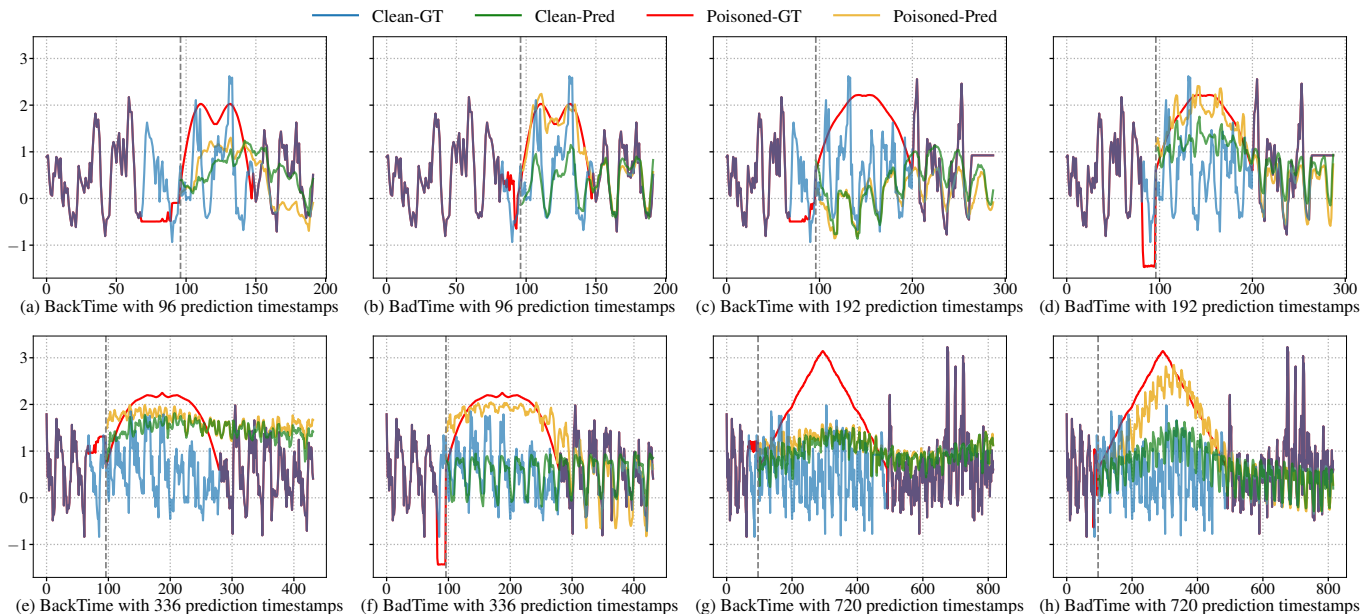


Fig. 4. Visualization of attack examples for BackTime and BadTime across four prediction lengths: 96, 192, 336, and 720.

TABLE V
FORECASTING PERFORMANCE AND ATTACK EFFECTIVENESS OF BENIGN, BACKTIME, AND BADTIME UNDER VARYING PREDICTION LENGTHS.

Horizon	Benign			BackTime [13]			BadTime (Ours)		
	MAE _c	MAE _{pa}	MAE _{pn}	MAE _c	MAE _{pa}	MAE _{pn}	MAE _c	MAE _{pa}	MAE _{pn}
96	0.424	0.781	0.432	0.448	0.750	0.439	0.421	0.376	0.429
192	0.464	0.848	0.476	0.474	0.768	0.455	0.459	0.465	0.468
336	0.470	0.904	0.484	0.512	0.781	0.480	0.474	0.467	0.479
720	0.493	0.960	0.509	0.510	0.857	0.501	0.508	0.505	0.516

2) *Robustness comparison to longer forecast lengths:* To assess the robustness of BadTime to longer forecast lengths, we conduct experiments on the ETTh1 dataset using the TimesNet model, gradually extending the prediction horizon from 96 to 192, 336, and 720. The experimental results are presented in Table V. Table V shows that the models trained by both BackTime and BadTime maintain competitive forecasting performance under four prediction lengths, remaining comparable to the Benign baseline. Table V also demonstrates that BadTime remains effective in backdooring MLTSF models across all four prediction lengths, even at 720. Notably, it reduces MAE_{pa} by nearly half compared to the SOTA BackTime, demonstrating superior effectiveness and establishing it as the first effective backdoor attack for MLTSF.

3) *Stealthiness comparison:* Next, we employ time series anomaly detectors USAD [16] and TranAD [17] to verify that BadTime’s data modifications are more imperceptible. Specifically, for each dataset, we first train the anomaly detection models on its clean training data, and then measure the models’ F1-score and Accuracy (ACC) on its poisoned validation set. Lower F1-score and ACC indicate that anomaly detectors struggle to distinguish between normal and modified inputs, reflecting better stealth of the modifications. Experiments are conducted on 6 MLTSF models across 7 datasets, with the results in Table VI. As shown, BadTime achieves

significantly lower F1-scores and ACC than BackTime across all datasets, confirming that BadTime’s data modifications are more stealthy than those introduced by the SOTA BackTime.

C. Ablation Analysis

In this subsection, we conduct ablation studies to evaluate the individual contribution of each key design in BadTime. We consider 5 ablation experiments for 4 data poisoning designs and the custom multi-objective loss in BadTime and evaluate them on the ETTh1 dataset and the TimesNet model. The following will explain the variants of its implementation:

- 1) **w/o-HPSS (Hybrid poisoned sample selection):** We removed the contrastive-guided sample selection strategy and randomly selected poisoned samples.
- 2) **w/o-GAT (GAT-based poisoned variable selection):** We replaced the GAT-based poisoned variable selection with random selection.
- 3) **w/o-Lag (Lag-aware trigger positioning):** We replaced our lag-aware trigger insertion strategy with two alternatives: random insertion (w/o-Lag) and fixed insertion at the input sequence end (Input End).
- 4) **w/o-Opt (Optimized trigger):** We disabled the trigger optimization mechanism and used either fixed initialized triggers (InitOnly) or fixed random (RandOnly).
- 5) **w/o-CustomObj (Customized objective):** We replaced our customized optimization objectives in Eq. 15 and 20 with the standard backdoor training objective in Eq. 1.

Table VII shows the results of the ablation study. We categorize the five key designs of BadTime into two types based on their contribution to attack effectiveness:

- 1) **Core designs essentials for backdoor success:** These designs directly determine whether the backdoor can succeed. Removing GAT-based variable selection (w/o-GAT) causes a sharp drop in MAE_{pa}, indicating that

TABLE VI

STEALTHINESS COMPARISON BETWEEN BACKTIME AND BADTIME USING ANOMALY DETECTION MODELS USAD AND TRANAD. LOWER F1 AND ACC INDICATE BETTER STEALTH AND BADTIME CONSISTENTLY PERFORMS BETTER.

Anomaly Detection	Backdoor Attacks	Models	ETTh1		ETTh2		ETtm1		ETtm2		Electricity		Weather		Exchange	
			F1-score	ACC	F1-score	ACC	F1-score	ACC	F1-score	ACC	F1-score	ACC	F1-score	ACC	F1-score	ACC
USAD	BackTime [13]	Autoformer	0.947	0.899	0.900	0.818	0.000	0.000	0.832	0.713	0.811	0.745	0.000	0.000	0.886	0.796
		Mamba	0.959	0.922	0.899	0.817	0.000	0.000	0.828	0.706	0.818	0.780	0.000	0.000	0.881	0.788
		TimesNet	0.955	0.915	0.910	0.835	0.000	0.000	0.818	0.692	0.863	0.732	0.000	0.000	0.883	0.791
		iTransformer	0.957	0.918	0.910	0.835	0.000	0.000	0.836	0.719	0.836	0.720	0.000	0.000	0.856	0.748
		TSMixer	0.943	0.892	0.910	0.835	0.000	0.000	0.807	0.676	0.814	0.662	0.000	0.000	0.855	0.747
		TimeMixer	0.930	0.869	0.906	0.828	0.000	0.000	0.841	0.726	0.825	0.708	0.000	0.000	0.856	0.748
		Average	0.949	0.903	0.906	0.828	0.000	0.000	0.827	0.705	0.828	0.725	0.000	0.000	0.870	0.770
	BadTime (Ours)	Autoformer	0.394	0.262	0.339	0.201	0.000	0.000	0.181	0.102	0.188	0.211	0.000	0.000	0.040	0.027
		Mamba	0.392	0.253	0.356	0.213	0.000	0.000	0.192	0.113	0.197	0.203	0.000	0.000	0.289	0.163
		TimesNet	0.381	0.266	0.348	0.202	0.000	0.000	0.185	0.106	0.182	0.198	0.000	0.000	0.276	0.150
		iTransformer	0.393	0.263	0.358	0.210	0.000	0.000	0.179	0.098	0.190	0.207	0.000	0.000	0.284	0.169
		TSMixer	0.380	0.254	0.335	0.208	0.000	0.000	0.189	0.109	0.188	0.192	0.000	0.000	0.278	0.150
		TimeMixer	0.392	0.265	0.350	0.213	0.000	0.000	0.183	0.104	0.190	0.208	0.000	0.000	0.284	0.161
		Average	0.389	0.261	0.348	0.208	0.000	0.000	0.185	0.105	0.189	0.203	0.000	0.000	0.242	0.137
TranAD	BackTime [13]	Autoformer	0.817	0.972	0.789	0.936	0.691	0.971	0.405	0.915	0.695	0.791	0.257	0.465	0.272	0.744
		Mamba	0.773	0.970	0.856	0.961	0.683	0.963	0.541	0.917	0.716	0.841	0.245	0.445	0.137	0.399
		TimesNet	0.796	0.974	0.806	0.959	0.647	0.971	0.560	0.922	0.748	0.818	0.235	0.513	0.266	0.661
		iTransformer	0.797	0.973	0.815	0.960	0.644	0.958	0.583	0.926	0.788	0.823	0.352	0.489	0.406	0.794
		TSMixer	0.773	0.962	0.841	0.977	0.637	0.951	0.516	0.925	0.697	0.785	0.211	0.439	0.293	0.761
		TimeMixer	0.813	0.955	0.827	0.949	0.632	0.632	0.555	0.929	0.763	0.839	0.346	0.550	0.397	0.729
		Average	0.795	0.968	0.822	0.957	0.656	0.908	0.527	0.922	0.735	0.816	0.274	0.484	0.295	0.681
	BadTime (Ours)	Autoformer	0.031	0.051	0.165	0.192	0.428	0.546	0.107	0.104	0.131	0.115	0.012	0.282	0.130	0.122
		Mamba	0.029	0.048	0.191	0.218	0.409	0.532	0.092	0.098	0.186	0.114	0.013	0.295	0.148	0.138
		TimesNet	0.036	0.053	0.188	0.214	0.409	0.532	0.102	0.100	0.193	0.149	0.009	0.282	0.130	0.122
		iTransformer	0.029	0.050	0.191	0.218	0.411	0.534	0.096	0.096	0.131	0.168	0.012	0.295	0.129	0.121
		TSMixer	0.035	0.049	0.188	0.214	0.373	0.503	0.108	0.105	0.192	0.152	0.011	0.288	0.130	0.122
		TimeMixer	0.034	0.054	0.184	0.211	0.382	0.511	0.097	0.099	0.155	0.122	0.013	0.291	0.127	0.119
		Average	0.032	0.051	0.185	0.211	0.402	0.526	0.100	0.100	0.165	0.137	0.012	0.289	0.132	0.124

TABLE VII

THE EXPERIMENTAL RESULTS FOR ABLATION ANALYSIS WITH THE BEST PERFORMANCE HIGHLIGHTED IN BOLD. HORIZONTAL LINES IN THE MIDDLE OF THE TABLE SEPARATE DIFFERENT ABLATION MODULES.

Metric	MAE _c	MAE _{pa}	MAE _{pn}	ACC _{USAD}	ACC _{TranAD}
Benign	0.424	0.781	0.432	\	\
BackTime [13]	0.448	0.750	0.439	0.915	0.974
BadTime	0.421	0.376	0.429	0.266	0.053
$\gamma = 0\%$	0.429	0.416	0.429	0.275	0.161
$\gamma = 25\%$	0.428	0.380	0.430	0.269	0.131
$\gamma = 50\%$	0.427	0.362	0.423	0.265	0.092
$\gamma = 75\%$	0.425	0.383	0.423	0.254	0.029
$\gamma = 100\%$	0.430	0.394	0.419	0.232	0.029
w/o-HPSS	0.428	0.406	0.429	0.268	0.134
w/o-GAT	0.444	0.529	0.446	0.263	0.007
w/o-Lag	0.429	0.397	0.428	0.263	0.057
Input End	0.421	0.393	0.425	0.263	0.051
InitOnly	0.425	0.397	0.427	0.263	0.084
RandOnly	0.477	0.511	0.438	0.263	0.051
w/o-CustomObj	0.481	0.578	0.485	0.263	0.051

selecting variables with strong influence on the target is key to effective attack. The optimized trigger clearly outperforms both fixed random (RandOnly) and fixed initialized (InitOnly) triggers, showing that initialization provides a good starting point while optimization further enhances effectiveness. Customized objectives are crucial because standard loss functions (w/o-CustomObj) tend to overlook the sparse target variables in a few poisoned samples, causing attack failure.

2) **Enhancement designs:** These designs enhance attack effectiveness and stealth. The hybrid poisoned sample selection significantly outperforms random selection (w/o-HPSS). We further analyze this component by varying the similarity mixing ratio γ from 0% to 100%. Table VII shows that attack effectiveness (MAE_{pa}) peaks at $\gamma = 50\%$ (0.362), outperforming both extremes ($\gamma = 0\%$: 0.416; $\gamma = 100\%$: 0.394) and the random baseline (w/o-HPSS: 0.406). This confirms our hypothesis: a balanced mix of label-similar and label-dissimilar samples prevents the model from attributing the target pattern to inherent data trends or opposing features, thereby strengthening the trigger–target association. Moreover, larger value of γ reduces anomaly detection accuracy, indicating improved stealth via smaller trigger perturbations. Complementing this, the lag-aware trigger positioning improves attack performance by placing the trigger at timestamps that maximize its influence on future target predictions (compare to “w/o-Lag” and “Input End”).

D. Robustness Analysis

Finally, we assess the robustness of the BadTime under varying experimental settings. In each case, only one parameter is modified while others follow the default configuration in the “Experimental Setup” subsection. Fig. 5(a) shows that our method remains effective even when only 1% of the training samples are poisoned. Increasing α_T introduces more poisoned samples, allowing the model to better learn the mapping between triggers and target patterns, thereby

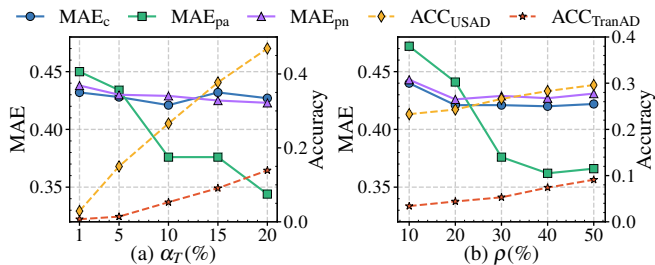


Fig. 5. Attack performance of BadTime under varying poisoning ratios (α_T) and trigger length ratios (ρ). Curves for MAE_c , MAE_{pa} , and MAE_{pn} should be read against the left y-axis (MAE; lower is better), whereas curves for ACC_{USAD} and ACC_{TranAD} should be read against the right y-axis (Accuracy; lower indicates better stealth).

enhancing attack performance. Although stealthiness slightly decreases, it remains at a low level overall. Fig. 5(b) shows that the BadTime remains effective even when the trigger length is only 10% of the input length. Meanwhile, although detection rates by ACC_{USAD} and ACC_{TranAD} slightly increase with ρ , they remain low overall. Table VIII shows that the attack performance of BadTime gradually declines as the number of target variables increases, due to the growing difficulty of steering more variables toward predefined patterns, yet it remains effective and stealthy even when targeting up to 70% of all variables. Table IX reveals that increasing the number of poisoned variables from 1 to 5 slightly reduces effectiveness. This occurs because the fixed total trigger length is spread across more variables, yielding shorter, fragmented segments that are harder for the model to learn. However, this same fragmentation also makes the trigger harder to detect, thereby improving stealth. Table X shows that BadTime maintains high attack effectiveness and stealthiness across all pattern types (visualized in Fig. 6), demonstrating its strong robustness to variations in target pattern shape.

TABLE VIII

PERFORMANCE OF BADTIME WHEN THE NUMBER OF TARGET VARIABLES VARIES. THE NOTATION $x/7$ INDICATES x TARGET VARIABLES OUT OF 7 TOTAL VARIABLES.

	MAE_c	MAE_{pa}	MAE_{pn}	ACC_{USAD}	ACC_{TranAD}
1/7	0.421	0.376	0.429	0.266	0.053
2/7	0.439	0.430	0.393	0.300	0.000
3/7	0.445	0.454	0.459	0.301	0.007
4/7	0.441	0.494	0.416	0.301	0.000
5/7	0.459	0.512	0.308	0.302	0.000

TABLE IX

PERFORMANCE OF BADTIME WHEN ATTACKING WITH DIFFERENT NUMBERS OF POISONED VARIABLES. THE NOTATION $x/7$ INDICATES x POISONED VARIABLES OUT OF 7 TOTAL VARIABLES.

	MAE_c	MAE_{pa}	MAE_{pn}	ACC_{USAD}	ACC_{TranAD}
1/7	0.423	0.363	0.433	0.363	0.078
2/7	0.421	0.376	0.429	0.266	0.053
3/7	0.423	0.401	0.429	0.265	0.022
4/7	0.429	0.440	0.432	0.265	0.007
5/7	0.436	0.448	0.435	0.265	0.000

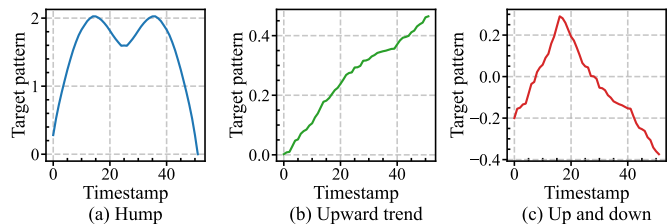


Fig. 6. The shapes of all the target patterns we evaluated in this paper.

TABLE X

ATTACK PERFORMANCE OF BADTIME TARGET THREE DIFFERENT TARGET PATTERN SHAPES.

	MAE_c	MAE_{pa}	MAE_{pn}	ACC_{USAD}	ACC_{TranAD}
Hump	0.421	0.376	0.429	0.266	0.053
Upward	0.425	0.375	0.429	0.291	0.050
Up-and-down	0.417	0.378	0.422	0.290	0.022

VI. CONCLUSION

In this paper, we have identified a very large gap in backdoor attacks in the MLTSF task. We have then pointed out three unique challenges for backdoor attacks in the MLTSF task: trigger signal attenuation due to long input sequences and the sparse backdoor signal under low poisoning ratio. Subsequently, we have addressed the above challenges and proposed BadTime, the first backdoor attack for the MLTSF task. Extensive experiments have shown that BadTime outperforms SOTA backdoor attacks for time series forecasting in both efficacy and stealth. We hope that our findings could alarm the time series community and encourage further research.

APPENDIX A

DESCRIPTIONS OF DATASETS

In this paper, we conduct extensive experiments on seven real-world MLTSF datasets: ETTh1 [9], ETTh2 [9], ETTm1 [9], ETTm2 [9], Electricity [8], Weather [8], and Exchange [8]. Table 2 presents the statistics for these datasets, as well as the train/validation/test split ratios used in our experiments. Below is a brief description of each dataset.

ETTh1 and ETTh2 datasets [9]. ETTh1 and ETTh2 are Electricity Transformer Temperature Hourly datasets from a Chinese power grid, each containing 17,420 timestamps, six transformer load measurements and oil temperature. The two datasets are recorded from different transformers.

ETTm1 and ETTm2 datasets [9]. ETTm1 and ETTm2 are 15-minute Electricity Transformer Temperature datasets collected from a Chinese power grid. Each dataset contains 69,680 timestamps, six transformer load measurements and oil temperature. The two datasets were recorded at different sites.

Electricity datasets [9]. The Electricity dataset comes from the UCI ‘‘ElectricityLoadDiagrams20112014’’² repository. It provides hourly electricity consumption for 321 customers over 26,304 timestamps, yielding a 321-variable series.

Weather dataset [8]. The Weather dataset contains 21 meteorological variables sampled every 10 minutes from 2010 to 2013, totaling 52,696 time steps.

²<https://archive.ics.uci.edu/dataset/321/electricityloadDiagrams20112014>

Exchange dataset [8]. Exchange dataset records daily exchange rates of eight currencies against the U.S. dollar (AUD, GBP, CAD, CHF, CNY, JPY, NZD, SGD) from 1990 to 2016, totaling 7,588 steps with eight variables.

TABLE XI
STATISTICS OF DATASETS

Dataset	Dimension	Length	Domain	Split (Train/Val/Test)
ETTh1, ETTh2	7	17,420	Electricity (1 hour)	6/2/2
ETTM1, ETTm2	7	69,680	Electricity (15 mins)	6/2/2
Electricity	321	26,304	Electricity (1 hour)	7/1/2
Weather	21	52,696	Environment (10 mins)	7/1/2
Exchange	8	7,588	Economic (1 day)	7/1/2

REFERENCES

- [1] M. R. Bendre, R. C. Thool, and V. R. Thool, "Big data in precision agriculture: Weather forecasting for future farming," in *2015 1st International Conference on Next Generation Computing Technologies (NGCT)*, 2015, pp. 744–750.
- [2] J. W. HANSEN, S. J. MASON, L. SUN, and A. TALL, "Review of seasonal climate forecasting for agriculture in sub-saharan africa," *Experimental Agriculture*, vol. 47, no. 2, p. 205–240, 2011.
- [3] A. Q. Md, S. Kapoor, C. J. AV, A. K. Sivaraman, K. F. Tee *et al.*, "Novel optimization approach for stock price forecasting using multi-layered sequential lstm," *Applied Soft Computing*, vol. 134, p. 109830, 2023.
- [4] T. B. Shahi, A. Shrestha, A. Neupane, and W. Guo, "Stock price forecasting with deep learning: A comparative study," *Mathematics*, vol. 8, no. 9, p. 1441, 2020.
- [5] W. Jiang and J. Luo, "Graph neural network for traffic forecasting: A survey," *Expert systems with applications*, vol. 207, p. 117921, 2022.
- [6] I. Lana, J. Del Ser, M. Velez, and E. I. Vlahogianni, "Road traffic forecasting: Recent advances and new challenges," *IEEE Intelligent Transportation Systems Magazine*, vol. 10, no. 2, pp. 93–109, 2018.
- [7] A. Vaswani, N. Shazeer, N. Parmar, J. Uszkoreit, L. Jones, A. N. Gomez, L. Kaiser, and I. Polosukhin, "Attention is all you need," *Advances in neural information processing systems*, vol. 30, 2017.
- [8] H. Wu, J. Xu, J. Wang, and M. Long, "Autoformer: Decomposition transformers with auto-correlation for long-term series forecasting," in *Advances in Neural Information Processing Systems*, M. Ranzato, A. Beygelzimer, Y. Dauphin, P. Liang, and J. W. Vaughan, Eds., vol. 34. Curran Associates, Inc., 2021, pp. 22 419–22 430. [Online]. Available: https://proceedings.neurips.cc/paper_files/paper/2021/file/bcc0d400288793e8bdcd7c19a8ac0c2b-Paper.pdf
- [9] H. Zhou, S. Zhang, J. Peng, S. Zhang, J. Li, H. Xiong, and W. Zhang, "Informer: Beyond efficient transformer for long sequence time-series forecasting," in *Proceedings of the AAAI conference on artificial intelligence*, vol. 35, no. 12, 2021, pp. 11 106–11 115.
- [10] Y. Liu, T. Hu, H. Zhang, H. Wu, S. Wang, L. Ma, and M. Long, "itransformer: Inverted transformers are effective for time series forecasting," *arXiv preprint arXiv:2310.06625*, 2023.
- [11] Y. Li, Y. Jiang, Z. Li, and S.-T. Xia, "Backdoor learning: A survey," *IEEE transactions on neural networks and learning systems*, vol. 35, no. 1, pp. 5–22, 2022.
- [12] Z. Chen, K. Dost, X. Zhu, X. Chang, G. Dobbie, and J. Wicker, "Targeted attacks on time series forecasting," in *Pacific-Asia conference on knowledge discovery and data mining*. Springer, 2023, pp. 314–327.
- [13] X. Lin, Z. Liu, D. Fu, R. Qiu, and H. Tong, "Backtime: Backdoor attacks on multivariate time series forecasting," *Advances in Neural Information Processing Systems*, vol. 37, pp. 131 344–131 368, 2024.
- [14] C. Chao, Z. Ma, and Z. Zhang, "Cyber resilience of three-phase unbalanced distribution system restoration under sparse adversarial attack on load forecasting," *arXiv preprint arXiv:2510.03635*, 2025.
- [15] Z. Zhang, W. Li, and H. Liu, "Multivariate time series forecasting by graph attention networks with theoretical guarantees," in *International Conference on Artificial Intelligence and Statistics*. PMLR, 2024, pp. 2845–2853.
- [16] J. Audibert, P. Michiardi, F. Guyard, S. Marti, and M. A. Zuluaga, "Usad: Unsupervised anomaly detection on multivariate time series," in *Proceedings of the 26th ACM SIGKDD international conference on knowledge discovery & data mining*, 2020, pp. 3395–3404.
- [17] S. Tuli, G. Casale, and N. R. Jennings, "Tranad: deep transformer networks for anomaly detection in multivariate time series data," *Proceedings of the VLDB Endowment*, vol. 15, no. 6, pp. 1201–1214, 2022.
- [18] S. Wang, S. Nepal, C. Rudolph, M. Grobler, S. Chen, and T. Chen, "Backdoor attacks against transfer learning with pre-trained deep learning models," *IEEE Transactions on Services Computing*, vol. 15, no. 3, pp. 1526–1539, 2020.
- [19] J. T. Holodnak, O. Brown, J. Matterer, and A. Lemke, "Backdoor poisoning of encrypted traffic classifiers," in *2022 IEEE International Conference on Data Mining Workshops (ICDMW)*. IEEE, 2022, pp. 577–585.
- [20] R. Ning, C. Xin, and H. Wu, "Trojanflow: A neural backdoor attack to deep learning-based network traffic classifiers," in *IEEE INFOCOM 2022-IEEE Conference on Computer Communications*. IEEE, 2022, pp. 1429–1438.
- [21] D. Ding, M. Zhang, Y. Huang, X. Pan, F. Feng, E. Jiang, and M. Yang, "Towards backdoor attack on deep learning based time series classification," in *2022 IEEE 38th International Conference on Data Engineering (ICDE)*. IEEE, 2022, pp. 1274–1287.
- [22] Y. Jiang, X. Ma, S. M. Erfani, and J. Bailey, "Backdoor attacks on time series: A generative approach," in *2023 IEEE Conference on Secure and Trustworthy Machine Learning (SaTML)*. IEEE, 2023, pp. 392–403.
- [23] C. Dong, Z. Sun, G. Bai, S. Piao, W. Chen, and W. E. Zhang, "TrojanTime: Backdoor attacks on time series classification," in *Pacific-Asia Conference on Knowledge Discovery and Data Mining*. Springer, 2025, pp. 154–166.
- [24] Y. Huang, M. Zhang, Z. Wang, W. Li, and M. Yang, "Revisiting backdoor attacks on time series classification in the frequency domain," in *Proceedings of the ACM on Web Conference 2025*, 2025, pp. 1795–1810.
- [25] Y. Jiang, X. Ma, S. M. Erfani, Y. Li, and J. Bailey, "End-to-end anti-backdoor learning on images and time series," *CoRR*, 2024.
- [26] H. Wang, Y. Mo, K. Xiang, N. Yin, H. Dai, B. Li, and S. Fan, "Csformer: Combining channel independence and mixing for robust multivariate time series forecasting," in *Proceedings of the AAAI Conference on Artificial Intelligence*, vol. 39, no. 20, 2025, pp. 21 090–21 098.
- [27] Y. Govindarajulu, A. Amballa, P. Kulkarni, and M. Parmar, "Targeted attacks on timeseries forecasting," *arXiv preprint arXiv:2301.11544*, 2023.
- [28] H. Han, M. Zhang, M. Hou, F. Zhang, Z. Wang, E. Chen, H. Wang, J. Ma, and Q. Liu, "Stgcn: A spatial-temporal aware graph learning method for poi recommendation," in *2020 IEEE International Conference on Data Mining (ICDM)*, 2020, pp. 1052–1057.
- [29] H. Wu, T. Hu, Y. Liu, H. Zhou, J. Wang, and M. Long, "Timesnet: Temporal 2d-variation modeling for general time series analysis," in *International Conference on Learning Representations*, 2023.
- [30] T. Zhou, Z. Ma, Q. Wen, X. Wang, L. Sun, and R. Jin, "FEDformer: Frequency enhanced decomposed transformer for long-term series forecasting," in *Proceedings of the 39th International Conference on Machine Learning*, ser. Proceedings of Machine Learning Research, K. Chaudhuri, S. Jegelka, L. Song, C. Szepesvari, G. Niu, and S. Sabato, Eds., vol. 162. PMLR, 17–23 Jul 2022, pp. 27 268–27 286. [Online]. Available: <https://proceedings.mlr.press/v162/zhou22g.html>
- [31] J. Benesty, J. Chen, Y. Huang, and I. Cohen, "Pearson correlation coefficient," in *Noise Reduction in Speech Processing*. Springer, 2009.
- [32] T. Huynh, D. Nguyen, T. Pham, and A. Tran, "Combat: Alternated training for effective clean-label backdoor attacks," in *Proceedings of the AAAI Conference on Artificial Intelligence*, vol. 38, no. 3, 2024, pp. 2436–2444.
- [33] K. Doan, Y. Lao, W. Zhao, and P. Li, "Lira: Learnable, imperceptible and robust backdoor attacks," in *Proceedings of the IEEE/CVF international conference on computer vision*, 2021, pp. 11 966–11 976.
- [34] T. A. Nguyen and A. Tran, "Input-aware dynamic backdoor attack," *Advances in Neural Information Processing Systems*, vol. 33, pp. 3454–3464, 2020.
- [35] A. Gu and T. Dao, "Mamba: Linear-time sequence modeling with selective state spaces," *arXiv preprint arXiv:2312.00752*, 2023.
- [36] S.-A. Chen, C.-L. Li, N. Yoder, S. O. Arik, and T. Pfister, "Tsmixer: An all-mlp architecture for time series forecasting," *arXiv preprint arXiv:2303.06053*, 2023.
- [37] S. Wang, H. Wu, X. Shi, T. Hu, H. Luo, L. Ma, J. Y. Zhang, and J. ZHOU, "Timemixer: Decomposable multiscale mixing for time series forecasting," in *International Conference on Learning Representations (ICLR)*, 2024.
- [38] C. J. Willmott and K. Matsuura, "Advantages of the mean absolute error (mae) over the root mean square error (rmse) in assessing average model performance," *Climate research*, vol. 30, no. 1, pp. 79–82, 2005.